



PREDICTION OF SEISMIC DAMAGE FOR BEAMS AND JOINT PANELS IN STEEL MOMENT FRAMES

S. Mukaide¹, S. Kuwahara² and M. Tada³

ABSTRACT

This paper considers a prediction method for seismic damage of individual members in a steel moment frame that forms a sway mechanism. In the proposed prediction method, seismic damage is estimated without using seismic response analysis, based on seismic input energy on the frame and restoring force characteristics of the members. The energy is distributed to cruciform subassemblages, which are employed as unit elements in the method. Maximum deformation and cumulative plastic deformation of the members (beams and joint panels) are calculated as seismic damage by assuming that cruciform subassemblages deform due to the dissipation of the energy in specified situations, respectively. The applicability of the proposed method is confirmed through comparison with results of numerical analysis.

Introduction

Members of structures must be designed with larger ductility capacity than the demand (based on the predicted seismic damage), in seismic design that permits plastic deformation. Many researchers study design problems from this perspective. For example, Ogawa (Nov. 2000) presented a seismic design procedure for estimating the ductility demand of beams in strong column - weak beam steel frames. The theoretical solution is obtained with equivalent single-degree-of-freedom systems. However, Ogawa did not present the respective deformations of beams and joint panels. It is quite possible that, not only beams, but also joint panels yield under severe earthquake loads. In such a case, the damage of the joint panel influences the beam connected to it. Therefore, it is necessary to evaluate the damage of beams taking into account the damage of joint panels.

The purpose of the present study was to propose a prediction method for the seismic damage of members (both beams and joint panels) in a steel moment frame that forms a sway mechanism. More specifically, the maximum deformation and cumulative plastic deformation of members are calculated by using seismic input energy on the frame and restoring force characteristics of the members, without employing earthquake response analysis. The seismic responses are varied considerably, because of the varied characteristics of individual earthquakes, even if the structure is the same. The calculated deformation approximates the average earthquake response in an attempt to represent the general behavior of the members during a severe earthquake. This paper demonstrates the accuracy of the

¹ Research Associate, Graduate School of Engineering, Osaka University, Suita City, Japan

² Associate Professor, Graduate School of Science and Technology, Kyoto Institute of Technology, Kyoto City, Japan

³ Associate Professor, Graduate School of Engineering, Osaka University, Suita City, Japan

estimated deformations using a comparison with numerical results. We expect that the method will provide a fundamental understanding of the ductility demand of beams and joint panels.

Subassemblage for Proposed Method

Force-Deformation Relationship of Members

In this paper, a moment steel frame that forms a sway mechanism is considered. A typical interior beam-column subassemblage of the frame is shown in Fig. 1. The cruciform subassemblage consists of upper and lower half columns, left and right half beams, and a joint panel. The subassemblage is used as a unit element in the prediction method. Therefore, in the first instance the force-deformation relationship of the subassemblage and the members is formulated.

The moments at a node that is an intersection point of column and beam centerlines are used in order to satisfy the equilibrium condition among the members as shown in Fig. 2 (Kuwahara, 1998). The sum of the column moments at the node, the sum of the beam moments at the node, and the joint panel moments at the node are equal, with

$${}_cM_U^* + {}_cM_L^* = {}_bM_L^* + {}_bM_R^* = {}_pM^* = M^* \quad (1)$$

where ${}_cM_U^*$ and ${}_cM_L^*$ are the moments of columns at the node, ${}_bM_L^*$, ${}_bM_R^*$ are the moments of beams at the node, and the moment of the joint panel at the node ${}_pM^*$. Using the moment at the node M^* , it is relatively straightforward to consider both the order of plastic hinge formation and the mechanism (beam-hinging mechanism or joint panel mechanism).

Inter-story drift angle R is defined as the total deformation in the subassemblage under the applied moment at the node. This deformation is divided into the column region, the beam region, and the joint panel as shown in Fig. 3:

$$R = {}_c\theta^* + {}_b\theta^* + {}_p\theta^* \quad (2)$$

where, ${}_c\theta^*$, ${}_b\theta^*$ and ${}_p\theta^*$ are the rotation at the node of the column region, the beam region and the joint panel, respectively. The rotation at the node of the beam region is equal to the rotations of the left and right beams:

$${}_b\theta^* = {}_b\theta_L^* = {}_b\theta_R^* \quad (3)$$

Formulation of the moment and rotation at the node is described in the appendix.

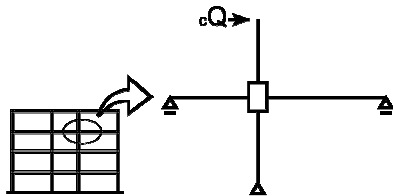


Figure 1. Cruciform subassemblage.

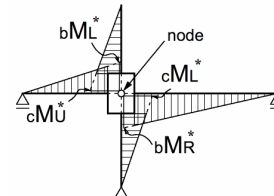


Figure 2. Column and beam moments at the node.

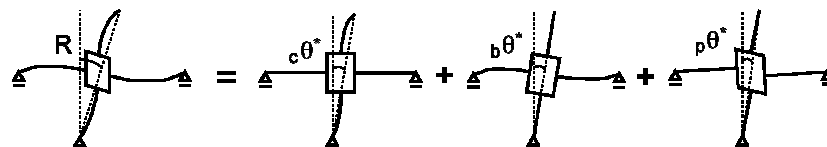


Figure 3. Deformation in subassemblage.

The columns are elastic because the frame forms a sway mechanism, and the beams and the individual joint panels are elasto-plastic (represented by a bi-linear model here). The assumed force-deformation relationship of the members is shown in Fig. 4. In this figure, ${}_cK^*$, ${}_bK^*_L$, ${}_bK^*_R$ and ${}_pK^*$ are the initial stiffness of the column region, the left beam, the right beam and the joint panel. ${}_b\alpha_L$, ${}_b\alpha_R$ and ${}_p\alpha$ are the second stiffness of the left and right beams and the joint panel. ${}_bM^*_{pL}$, ${}_bM^*_{pR}$ and ${}_pM^*_p$ are the full plastic moments at the node in the left and right beams and the joint panel. For simplicity, in this paper it is assumed that the formation of a plastic hinge in the left beam precedes the one in the right beam.

Force-Deformation Relationship of Subassemblage

The subassemblage is modeled as tetra-linear by connecting the members in series as shown in Fig. 4. M^*_1 , M^*_2 and M^*_3 are moments at the node when these moments reach the first, second and third corner points, respectively. K_1 , K_2 , K_3 and K_4 are the stiffness of the model.

Let us consider the order of plasticity in the members to formulate the model. ${}_bM^*_{pL}$ and ${}_bM^*_{pR}$ are derived from Eqs. 1 and 3.

$${}_bM^*_L = \frac{{}_bK^*_L}{{}_bK^*_L + {}_bK^*_R} \cdot M^* = {}_bk_L \cdot M^* \quad (4)$$

$${}_bM^*_R = \frac{{}_bK^*_R}{{}_bK^*_L + {}_bK^*_R} \cdot M^* = {}_bk_R \cdot M^* \quad (5)$$

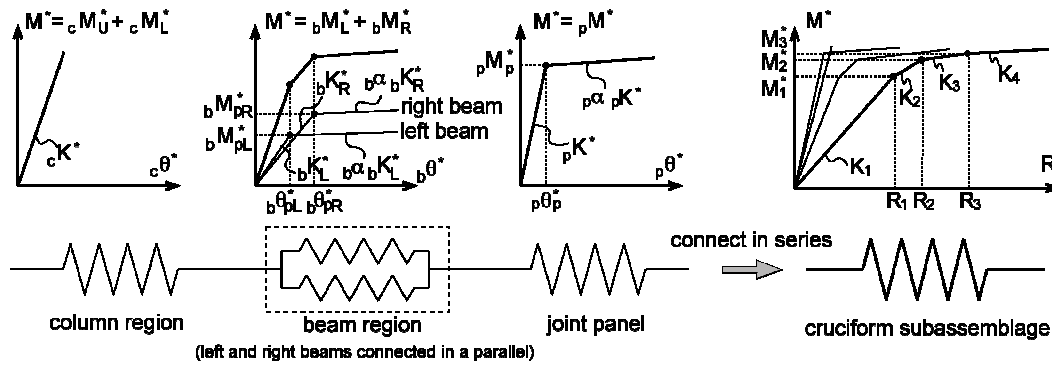


Figure 4. Force-deformation relationship of members and subassemblage.

When the plastic moment is reached at the left beam (right beam is elastic), M^* can be derived.

$$M^* = \frac{{}_bM^*_{pL}}{{}_bk_L} \quad (6)$$

Until the moment reaches the full plastic value in the right beam, the left beam moment at the node increases according to the second stiffness. However, this increase is small, and M^* is found by neglecting it.

$$M^* = {}_bM^*_{pL} + {}_bM^*_{pR} = \sum {}_bM^*_p \quad (7)$$

The mechanisms of the subassemblage are formed when $M^* = {}_pM^*_p$ or $M^* = \sum {}_bM^*_p$. M^*_1 , M^*_2 and M^*_3 are given by the values from Eqs. 6 and 7 and ${}_pM^*_p$ in ascending order.

When all of the members are elastic, the initial stiffness of the model is given by

$$\mathbf{M}^* = \mathbf{K}_1 \mathbf{R}, \quad \mathbf{K}_1 = \left(\frac{1}{cK^*} + \frac{1}{bK_L^* + bK_R^*} + \frac{1}{pK^*} \right)^{-1} \quad (8), (9)$$

The stiffness of the subassemblage is obtained by replacing the stiffness of the members that have formed plastic hinges with the second stiffness in Eq. 9.

Prediction Method for Seismic Damage

Seismic Input Energy

It is widely recognized that seismic input energy on a frame is scarcely affected by the strength and the type of the restoring force. Hence, seismic input energy is given by assuming the magnitude of the earthquake at the time the frame is designed. Damage-causing earthquake input energy \mathbf{E}_{dm} is applied as seismic input energy (Ogawa Apr., 2000) in this paper. \mathbf{E}_{dm} is defined as the maximum response of the sum of elastic strain energy \mathbf{E}_e and the energy dissipated by plastic deformation \mathbf{E}_p . Kinematic energy is not included in this definition.

$$\mathbf{E}_{dm} = (\mathbf{E}_e + \mathbf{E}_p)_{\max} \quad (10)$$

An example of the response of $(\mathbf{E}_e + \mathbf{E}_p)/\mathbf{E}_{dm}$ is shown in Fig. 5. The maximum response of $\mathbf{E}_e + \mathbf{E}_p$ (= \mathbf{E}_{dm}) subtracted by \mathbf{E}_e stored when plastic deformation occurs last is \mathbf{E}_p , as in Fig. 5. The value of \mathbf{E}_e varies according to the deformation if the model of the frame is not elasto-plastic. The value of \mathbf{E}_e is approximated to elastic strain energy when a mechanism is formed.

$$\mathbf{E}_e \cong \mathbf{E}_y \quad (11)$$

A fishbone-shaped frame such as that shown in Fig. 6 is employed as it is the simplest model of a multi-story frame. The fishbone-shaped frame consists of cruciform subassemblages. Considering seismic input energy on each story (each subassemblage in the fishbone-shaped frame), ${}_i\mathbf{E}_{dm}$ is defined as the sum of the elastic strain energy ${}_i\mathbf{E}_e$ and the energy dissipated by plastic deformation ${}_i\mathbf{E}_p$ of the i -th story of an n -story-high frame when $\mathbf{E}_e + \mathbf{E}_p$ reach \mathbf{E}_{dm} . $i = 0$ represents the bottom of the column of the lowest story, as in Fig. 6.

$$\mathbf{E}_{dm} = \sum_{i=0}^n {}_i\mathbf{E}_{dm} \quad (12)$$

$${}_i\mathbf{E}_{dm} = {}_i\mathbf{E}_e + {}_i\mathbf{E}_p \cong {}_i\mathbf{E}_y + {}_i\mathbf{E}_p \quad (13)$$

For simplicity, this paper deals with a frame that has an optimum strength distribution in which the cumulative plastic deformations of all stories, except the lowest, are the same. Since the purpose of this study is not to investigate the damage to the column of the lowest story, the condition where ${}_0\mathbf{E}_{dm}$ is known, is employed. As a result, ${}_i\mathbf{E}_{dm}$ is proportional to the strength of each story.

$$\left. \begin{aligned} {}_i\mathbf{E}_{dm} &= \sum_{i=1}^n {}_i r_i \mathbf{E}_{dm} \\ {}_1 r + \dots + {}_i r + \dots + {}_n r &= 1 \\ \frac{{}_1 r}{{}_1 M_p^*} &= \dots = \frac{{}_i r}{{}_i M_p^*} = \dots = \frac{{}_n r}{{}_n M_p^*} \end{aligned} \right\} \quad (14)$$

${}_i M_p^*$ is the moment at the node on the i -th story when the mechanism is formed and ${}_i\mathbf{E}_{dm}$ is derived as described above. In this case, behavior caused by interaction of each story is not considered, and hence, that each cruciform subassemblage is treated as a unit element for the prediction method. The subscript "i" is omitted in the following section.

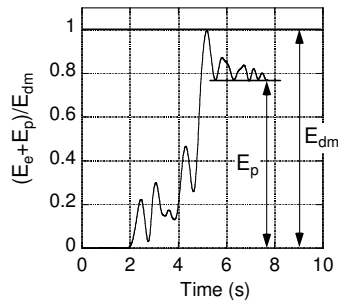


Figure 5. Example of energy response.

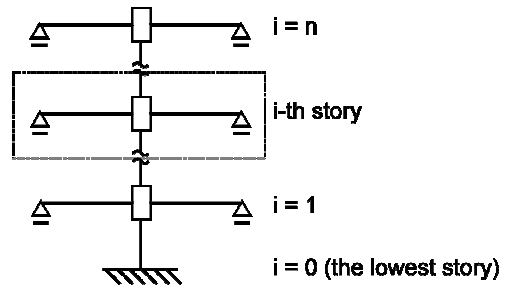


Figure 6. Fishbone-shaped frame.

Maximum Deformation

When deformation of a subassembly reaches a maximum, the deformations of component members usually reach maximum levels under a severe earthquake. In order to estimate the maximum deformation of members, we consider two kinds of processes that cause deformation of a subassembly to reach the maximum, as shown in Fig. 7. One is a situation in which the subassembly absorbs the maximum seismic energy as it deforms in one direction. The other is a situation where it absorbs a small amount of seismic energy after it deforms repeatedly in one direction. Generally, deformation of a reinforced concrete structure - when the degrading tri-linear model is used - reaches a maximum in the former situation, otherwise it is almost equal to the deformation in the latter situation (Nakamura 1998). Nakamura also stated that it is adequate to employ the corner point of the model when the structure reaches lateral strength in the inverse direction as a starting point in the former situation.

When the subassembly deforms in one direction, the response of $E_e + E_p$ varies from one of the relative maximums to the next. This term is called a half-cycle. In order to estimate the maximum deformation, it is adequate to assume that the maximum increment of $E_e + E_p$ during a half-cycle ΔE_1 is $0.25E_{dm}$ (Ogawa Jun., 2000).

Based on the aforementioned description, the maximum deformation of members in the prediction method is calculated by assuming that the subassembly deforms from the first corner point (the moment at the node is M^*_1) in the inverse direction while absorbing ΔE_1 , as shown in Fig. 8. In this case, the subassembly deforms over the first corner point by releasing the stored elastic strain energy. The maximum moment at the node M^*_{max} is calculated.

$$\left. \begin{aligned} M^*_{max} &= \sqrt{2\Delta E_1 \cdot K_2 + (M^*_1)^2} & \Delta E_1 < E_{2nd} \\ M^*_{max} &= \sqrt{2(\Delta E_1 - E_{2nd}) \cdot K_3 + (M^*_2)^2} & E_{2nd} \leq \Delta E_1 < E_{3rd} \\ M^*_{max} &= \sqrt{2(\Delta E_1 - E_{3rd}) \cdot K_4 + (M^*_3)^2} & E_{3rd} \leq \Delta E_1 \end{aligned} \right\} \quad (15)$$

where E_{2nd} and E_{3rd} are the energy required to deform through the second and third corner point, respectively. The maximum deformation of the beam region and the joint panel is calculated by using restoring force characteristics, as shown in Fig. 4.

$$\left. \begin{aligned}
 {}_b\theta_{\max}^* &= \frac{M_{\max}^*}{{}_bK_L + {}_bK_R} & M_{\max}^* &< \frac{{}_bM_{pL}^*}{{}_bK_L} \\
 {}_b\theta_{\max}^* &= \frac{M_{\max}^* - (1 - {}_b\alpha_L) {}_bM_{pL}^*}{{}_b\alpha_L {}_bK_L + {}_bK_R} & \frac{{}_bM_{pL}^*}{{}_bK_L} &\leq M_{\max}^* < \sum {}_bM_p^* \\
 {}_b\theta_{\max}^* &= \frac{M_{\max}^* - (1 - {}_b\alpha_L) {}_bM_{pL}^* - (1 - {}_b\alpha_R) {}_bM_{pR}^*}{{}_b\alpha_L {}_bK_L + {}_b\alpha_R {}_bK_R} & \sum {}_bM_p^* &\leq M_{\max}^*
 \end{aligned} \right\} \quad (16)$$

$$\left. \begin{aligned}
 {}_p\theta_{\max}^* &= \frac{M_{\max}^*}{{}_pK^*} & M_{\max}^* &< {}_pM_p^* \\
 {}_p\theta_{\max}^* &= \frac{M_{\max}^* - (1 - {}_p\alpha) {}_pM_p^*}{{}_p\alpha {}_pK^*} & {}_pM_p^* &\leq M_{\max}^*
 \end{aligned} \right\} \quad (17)$$

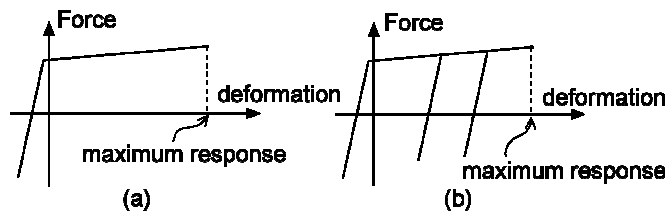


Figure 7. Situations when maximum response occurs

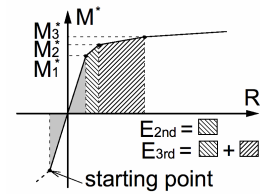


Figure 8. Maximum deformation in prediction method.

Cumulative Plastic Deformation

Calculation of the cumulative plastic deformation as the subassembly deforms under seismic excitation is complicated due to the irregularities that arise in deformation. In the prediction method, the deformation in the following situation is regarded as cumulative plastic deformation of members; the subassembly deforms with the same amplitude in both positive and negative directions, absorbing the seismic energy $\Delta E_{2m-1} + \Delta E_{2m}$ during two half-cycles (one cycle), where ΔE_j is the j -th largest energy increment during a half-cycle. Each single cycle does not continue to the next one, and each occurs I times as shown in Fig. 9. In this situation, it is easier to calculate the cumulative plastic deformation of members even though the model is tetra-linear. We assume that ΔE_j decreases linearly if ΔE_j is arranged in order of magnitude despite actual process as shown in Fig. 10(a). In this case, ΔE_{2m-1} differs from ΔE_{2m} , but the subassembly is considered to absorb the average of both energies during each half-cycle.

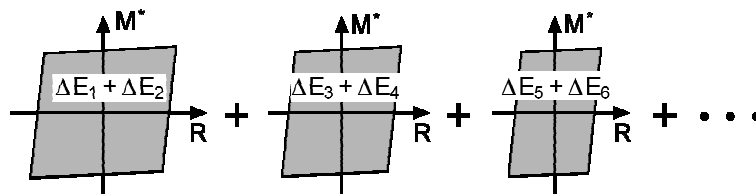


Figure 9. Deformation of subassembly for predicting cumulative plastic deformation

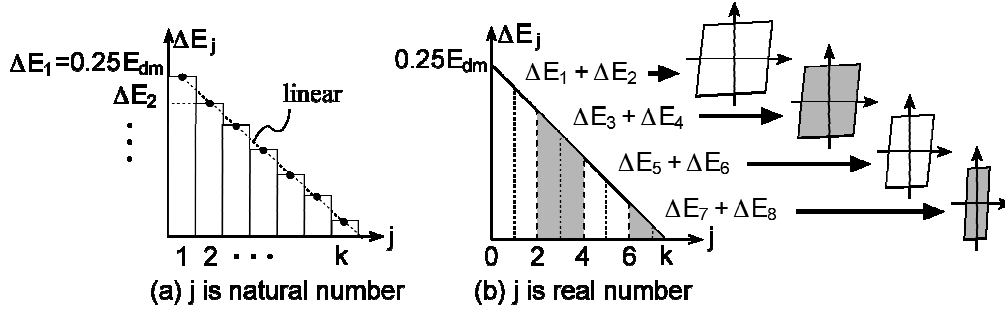


Figure 10. Half-cycle energy in order of magnitude.

For simplicity, we assume j is a real number, although it is actually a natural number. The sum of ΔE_j is derived by ignoring the elastic strain energy, which is stored during previous half-cycles. Thus,

$$E_p = \int_0^k \Delta E_j dj \quad (18)$$

where k is the total number of times the plastic deformations occur and ΔE_j is derived from assuming $\Delta E_j = 0$ when $j = 0$ as shown in Fig. 10(b).

$$\Delta E_j = 0.25E_{dm} \left(1 - \frac{j}{k}\right) \quad (19)$$

from Eqs. 13, 18 and 19,

$$\Delta E_{2m-1} + \Delta E_{2m} = \int_{2m-2}^{2m} \Delta E_j dj = \frac{k-2m+1}{2k} E_{dm}, \quad k = 8 \left(1 - \frac{E_y}{E_{dm}}\right) \quad (20), (21)$$

The amplitude of the moment at the node of the m -th cycle $M^*_{(m)}$ is defined in Fig. 11. $M^*_{(m)}$ is derived from $\Delta E_{2m-1} + \Delta E_{2m}$.

$$\left. \begin{aligned} M^*_{(m)} &= \frac{\Delta E_{2m-1} + \Delta E_{2m}}{2 \left(-\frac{M^*_1}{K_1} + \frac{M^*_1}{K_2} \right)} + 2M^*_1 && \Delta E_{2m-1} + \Delta E_{2m} < E_{p2} \\ M^*_{(m)} &= \frac{\Delta E_{2m-1} + \Delta E_{2m} + \left\{ -\frac{(M^*_1)^2}{K_1} + \frac{(M^*_1)^2 - (M^*_2)^2}{K_2} + \frac{(M^*_2)^2}{K_3} \right\}}{2 \left(-\frac{M^*_1}{K_1} + \frac{M^*_1 - M^*_2}{K_2} + \frac{M^*_2}{K_3} \right)} && E_{p2} \leq \Delta E_{2m-1} + \Delta E_{2m} < E_{p3} \\ M^*_{(m)} &= \frac{\Delta E_{2m-1} + \Delta E_{2m} + \left\{ -\frac{(M^*_1)^2}{K_1} + \frac{(M^*_1)^2 - (M^*_2)^2}{K_2} + \frac{(M^*_2)^2 - (M^*_3)^2}{K_3} + \frac{(M^*_3)^2}{K_4} \right\}}{2 \left(-\frac{M^*_1}{K_1} + \frac{M^*_1 - M^*_2}{K_2} + \frac{M^*_2 - M^*_3}{K_3} + \frac{M^*_3}{K_4} \right)} && E_{p3} \leq \Delta E_{2m-1} + \Delta E_{2m} \end{aligned} \right\} (22)$$

where E_{p2} and E_{p3} are the energy when the amplitude of moment at the node reaches the second and third corner point.

$$\left. \begin{aligned} E_{p2} &= 4M_1^*(M_2^* - M_1^*) \left(-\frac{1}{K_1} + \frac{1}{K_2} \right) \\ E_{p3} &= 4M_1^*(M_3^* - M_1^*) \left(-\frac{1}{K_1} + \frac{1}{K_2} \right) + 4M_2^*(M_3^* - M_2^*) \left(-\frac{1}{K_2} + \frac{1}{K_3} \right) \end{aligned} \right\} \quad (23)$$

The plastic deformation of the left and right beams and the joint panel during one cycle is calculated with the force-deformation relationship.

$$\left. \begin{aligned} {}_b\theta_{pL(m)}^* &= 0 & M_{(m)}^* &< \frac{2{}_bM_{pL}^*}{{}_bK_L} \\ {}_b\theta_{pL(m)}^* &= \frac{2M_{(m)}^* - \frac{4{}_bM_{pL}^*}{{}_bK_L}}{{}_b\alpha_L{}_bK_L + {}_bK_R^*} & \frac{2{}_bM_{pL}^*}{{}_bK_L} &\leq M_{(m)}^* < 2\sum {}_bM_p^* \\ {}_b\theta_{pL(m)}^* &= \frac{2M_{(m)}^* - 4\left\{ \sum {}_bM_p^* + {}_b\alpha_R{}_bK_R^* ({}_b\theta_{pL}^* - {}_b\theta_{pR}^*) \right\}}{{}_b\alpha_L{}_bK_L + {}_b\alpha_R{}_bK_R^*} & 2\sum {}_bM_p^* &\leq M_{(m)}^* \end{aligned} \right\} \quad (24)$$

$$\left. \begin{aligned} {}_b\theta_{pR(m)}^* &= 0 & M_{(m)}^* &< 2\sum {}_bM_p^* \\ {}_b\theta_{pR(m)}^* &= \frac{2M_{(m)}^* - 4\left\{ \sum {}_bM_p^* + {}_b\alpha_L{}_bK_L^* ({}_b\theta_{pR}^* - {}_b\theta_{pL}^*) \right\}}{{}_b\alpha_L{}_bK_L + {}_b\alpha_R{}_bK_R^*} & 2\sum {}_bM_p^* &\leq M_{(m)}^* \end{aligned} \right\} \quad (25)$$

$$\left. \begin{aligned} {}_p\theta_{p(m)}^* &= 0 & M_{(m)}^* &< 2{}_pM_p^* \\ {}_p\theta_{p(m)}^* &= \frac{2M_{(m)}^* - 4{}_pM_p^*}{{}_p\alpha{}_pK^*} & 2{}_pM_p^* &\leq M_{(m)}^* \end{aligned} \right\} \quad (26)$$

Hence, the cumulative plastic deformation of the left and right beams and the joint panel is derived.

$$\sum {}_b\theta_{pL}^* = \sum_{m=1}^I {}_b\theta_{pL(m)}^*, \quad \sum {}_b\theta_{pR}^* = \sum_{m=1}^I {}_b\theta_{pR(m)}^*, \quad \sum {}_p\theta_p^* = \sum_{m=1}^I {}_p\theta_{p(m)}^* \quad (27), (28), (29)$$

where I is the number of the cycle and is obtained by rounding-up $k/2$ to the nearest natural number.

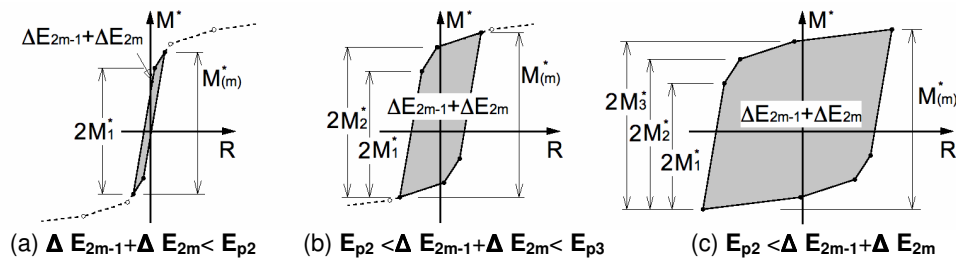


Figure 11. Amplitude of moment during each cycle.

Verification of Prediction Method

Subject Frame and Analysis Conditions

The model is a fishbone-shaped frame as shown in Fig. 6. To investigate the seismic damage of members used together that have various ratios of strength and stiffness, steel moment frames are designed by separating stiffness from strength, despite these being connected in reality. The stiffness of the frame is determined so that the inter-story drift angle of each story is 1/200 when seismic design

forces of Level 1 (as defined by the Japanese code) are applied. The strength of the frame is determined in order that a collapse mechanism is formed when ultimate horizontal bearing forces of Level 2 (as defined by the Japanese code) are applied.

The model parameters are the number of stories, the base shear factor (C_B), the ratios of strength and stiffness between the beam region and joint panel (${}_pM_p^*/\Sigma {}_bM_p^*$ and ${}_pK^*/{}_bK^*$), and the ratios of strength and stiffness between the left and right beams (${}_bM_{pL}^*/{}_bM_{pR}^*$ and ${}_bk_L$), as shown in Table 1. Each story of the frame has the same value for these parameters, except for C_B . In this case, ratios of energy, strength and stiffness are the same among the stories of a frame, and consequently, the predicted deformation is also the same for all frames. In Table 1, the underlined number is the combination of the parameters for a standard case. One of the parameters, C_B , ${}_bk_L$, ${}_bM_{pL}^*/{}_bM_{pR}^*$ and ${}_bK_L^*/{}_bK_R^*$ changes under the condition that the others remain constant. The computed fundamental periods are 0.98 and 1.77 s for the 4- and 8-story frames, respectively, irrespective of other parameters.

The frames were analyzed using the program CLAP.f (Ogawa and Tada 1994), which features inelastic modeling and geometric non-linearities. Three kinds of earthquakes, El Centro 1940 NS, Taft 1952 EW and NTTB3 1995 NS, are employed in the numerical analyses. These are scaled in such that the velocity equivalent of $E_{dm} (= (2g E_{dm}/W)^{0.5}$, g is the gravity acceleration, W is total weight of frame) corresponds to 1.5 m/s, by conducting repeated analyses. Other conditions of the analyses were described elsewhere by the authors (2002).

Table 1. Analysis parameters.

number of stories		n	4, 8
base shear factor		C_B	<u>0.14</u> , 0.19, 0.24
ratio of strength	between beam region and joint panel	${}_pM_p^*/\Sigma {}_bM_p^*$	0.5, 0.6, 0.8, 0.9, 1.0, 1.1, 1.2, 1.3, 1.4, 1.5
	between left and right beams	${}_bM_{pL}^*/{}_bM_{pR}^*$	0.50, 0.67, <u>1.00</u>
ration of stiffness	between beam region and joint panel	${}_pK^*/{}_bK^*$	1.0, <u>2.0</u> , 3.0
	between left and right beams	${}_bk_L$	<u>0.5</u> , 0.6, 0.7

Comparison between Response Analysis and Prediction Method

A large number of earthquake response analyses were conducted employing the aforementioned conditions. The comparison between these analyses and the predictions are shown in Figs. 12 to 15 and are example results of the results for 4-story frames. Figs. 12 to 13 are diagrams showing the maximum deformation of the beam region and joint panel (${}_b\theta_{max}^*$ and ${}_p\theta_{max}^*$) versus the strength ratio between the beam region and joint panel (${}_pM_p^*/\Sigma {}_bM_p^*$). Figs. 14 to 15 are diagrams showing the cumulative plastic deformations of the left beam and joint panel ($\Sigma {}_b\theta_{pL}^*$ and $\Sigma {}_p\theta^*$) versus ${}_pM_p^*/\Sigma {}_bM_p^*$. These figures clearly show the four points plotted for each parameter as the response for each story. The average line is plotted to show the tendency of the distributions of the analytical data, and the prediction line is also plotted.

It was found that C_B and ${}_pM_p^*/\Sigma {}_bM_p^*$ affect the response deformation of members, as is widely recognized. When the value of ${}_bM_{pL}^*/{}_bM_{pR}^*$ and ${}_bk_L$ differs from the standard case, implying that the formation of a plastic hinge in the left beam precedes that forming in the right beam, where $\Sigma {}_b\theta_{pL}^*$ is larger than $\Sigma {}_b\theta_{pR}^*$. In such a case, deformation of the joint panel tends to be smaller than the standard case. ${}_pK^*/{}_bK^*$ affect response deformation when both the beams and joint panel yield. Similarly, the

predicted deformations are in good agreement with the mean values obtained from the response analysis, which exhibits the tendency described above.

Conclusions

This paper proposed a prediction method for the seismic damage of beams and joint panels. In the method, the maximum and cumulative plastic deformations of each member were estimated based on the seismic energy applied to the frame and the force-deformation relationship of the members. Unlike other methods, the proposed method considers the stiffness of members and the order in which plastic hinges are formed by two beams that connect at the same node.

The large number of response analyses that were conducted, each with varying ratios of strength and stiffness of members as parameters, revealed that each parameter affects the deformation response. Moreover, the applicability of the proposed method was confirmed through comparisons with analytical results, which corroborated the finding well regardless of the parameters values.

Appendix

In a cruciform subassembly, the moment and rotation at the nodes of members are approximated. The column moment at the node ${}_c\mathbf{M}^*_U$, ${}_c\mathbf{M}^*_L$, the beam moment at the node ${}_b\mathbf{M}^*_L$, ${}_b\mathbf{M}^*_R$ and the joint panel moment at the node ${}_p\mathbf{M}^*$ are defined as follows:

$${}_c\mathbf{M}^*_U = {}_c\mathbf{M}_U + {}_c\mathbf{Q}_U \frac{d_b}{2} = \frac{{}_c\mathbf{M}_U}{1 - d_b/H_U}, \quad {}_c\mathbf{M}^*_L = {}_c\mathbf{M}_L + {}_c\mathbf{Q}_L \frac{d_b}{2} = \frac{{}_c\mathbf{M}_L}{1 - d_b/H_L} \quad (\text{A1.a}), (\text{A1.b})$$

$${}_b\mathbf{M}^*_L = {}_b\mathbf{M}_L + {}_b\mathbf{Q}_U \frac{d_c}{2} = \frac{{}_b\mathbf{M}_L}{1 - d_c/L_L}, \quad {}_b\mathbf{M}^*_R = {}_b\mathbf{M}_R + {}_b\mathbf{Q}_R \frac{d_c}{2} = \frac{{}_b\mathbf{M}_R}{1 - d_c/L_R} \quad (\text{A1.c}), (\text{A1.d})$$

$${}_p\mathbf{M}^* = {}_p\mathbf{M} + ({}_b\mathbf{Q}_L + {}_b\mathbf{Q}_R) \frac{d_c}{2} + ({}_c\mathbf{Q}_U + {}_c\mathbf{Q}_L) \frac{d_b}{2} = \frac{{}_p\mathbf{M}}{2 - d_b/H_L - d_b/H_L - d_c/L_L - d_c/L_R} \quad (\text{A1.e})$$

where ${}_c\mathbf{M}_U$, ${}_c\mathbf{M}_L$ = column moments at the surface of the beam, ${}_b\mathbf{M}_L$, ${}_b\mathbf{M}_R$ = beam moments at the surface of the column, and ${}_p\mathbf{M}$ = joint panel moment. H_U and H_L are the upper and lower story height, L_L and L_R are the width of left and right bays, d_c and d_b are the depth of the column and the beam.

The column rotations at the node ${}_c\theta^*_U$, ${}_c\theta^*_L$, the beam rotations at the node ${}_b\theta^*_L$, ${}_b\theta^*_R$ and the joint panel rotation at the node ${}_p\theta^*$ is defined as follows:

$${}_c\theta^*_U = (1 - d_b/H_U) {}_c\theta_U, \quad {}_c\theta^*_L = (1 - d_b/H_L) {}_c\theta_L \quad (\text{A2.a}), (\text{A2.b})$$

$${}_b\theta^*_L = (1 - d_c/L_L) {}_b\theta_L, \quad {}_b\theta^*_R = (1 - d_c/L_R) {}_b\theta_R \quad (\text{A2.c}), (\text{A2.d})$$

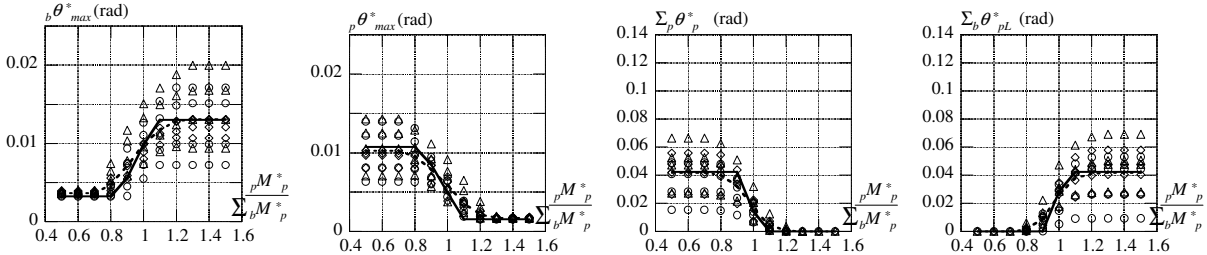
$${}_p\theta^* = \frac{2 - d_b/H_L - d_b/H_L - d_c/L_L - d_c/L_R}{2} {}_p\theta \quad (\text{A2.e})$$

where ${}_c\theta_U$, ${}_c\theta_L$ = column rotations at the surface of the beam, ${}_b\theta_L$, ${}_b\theta_R$ = beam rotations at the surface of the column and ${}_p\theta$ = joint panel rotation.

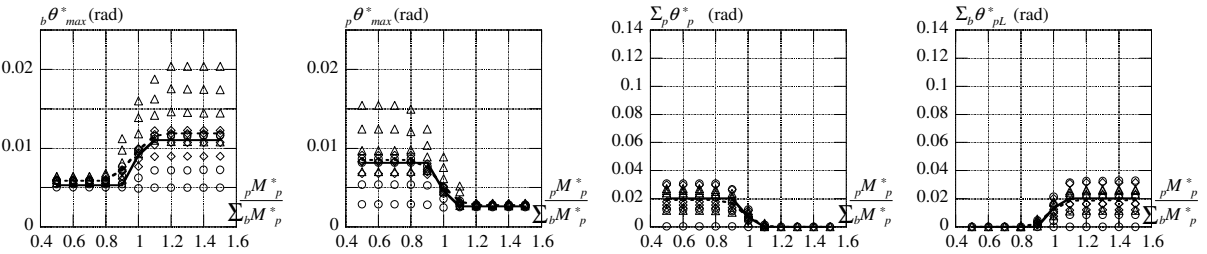
References

Kuwahara, S. and Inoue, K. (1998) "An approximate calculation for the plastic collapse load of the rigid frame considering joint panels," *Journal of Structural Engineering, AIJ*, Vol. 42B, 441-449, (in Japanese)

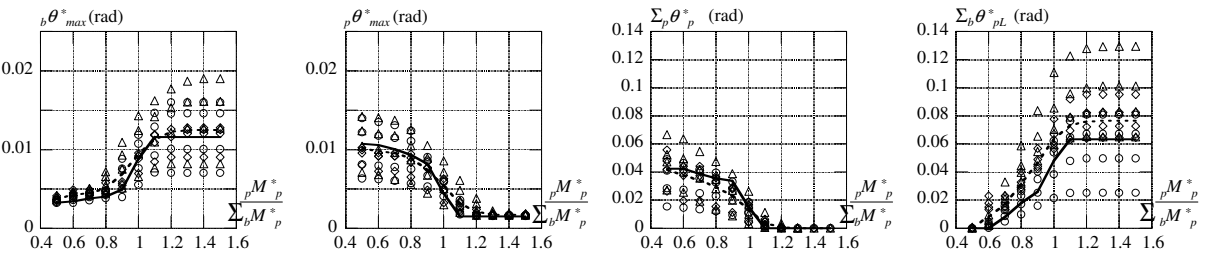
- Mukaide, S., Kuwahara, S. and Jikumaru, H. (2002) "Seismic damage distribution of beams and joint panels in steel moment frame," *Steel Construction Engineering, JSSC*, Vol. 9, No. 35, 55-64, (in Japanese)
- Nakamura, T., Hori, N. and Inoue, N. (1998) "Estimation method of maximum displacement of RC structures considering energy input process of ground motions," *Journal of Structural Engineering, AIJ*, Vol. 44B, 359-368, (in Japanese)
- Ogawa, K. and Tada, M. (1994) "Computer program for static and dynamic analysis of steel frames considering the deformation of joint panel," *Proceeding of the 17th Symposium on Computer Technology of Information, System and Applications, AIJ*, 79-84, (in Japanese)
- Ogawa, K., Inoue, K. and Nakashima, M. (Apr., 2000), "A study on earthquake input energy causing damages in structures," *Journal of Structural and Construction Engineering, AIJ*, No. 530, 177-184, (in Japanese)
- Ogawa, K. (Jun., 2000), "Earthquake input energy during half-cycle of vibration and maximum seismic response of bilinear systems," *Journal of Structural and Construction Engineering, AIJ*, No. 532, 185-192, (in Japanese)
- Ogawa, K., Inoue, K., Nakashima, M. and Sawaizumi, S. (Nov., 2000), "Ductility demand of members in steel moment frame s sustaining beam-hinging mechanism," *Journal of Structural and Construction Engineering, AIJ*, No. 537, 121-128, (in Japanese)



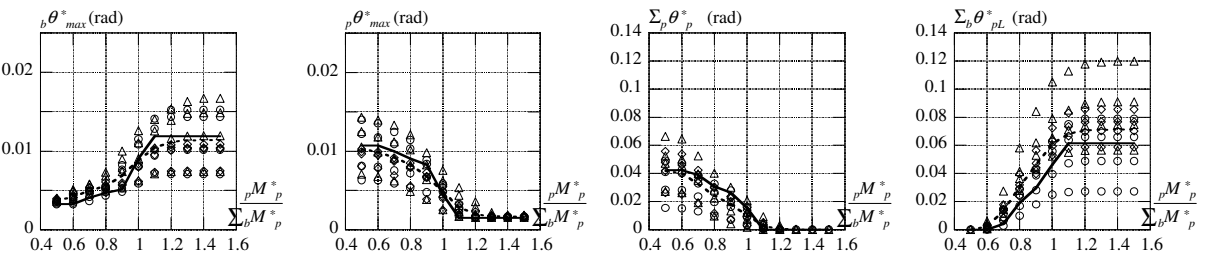
(a) Standard Case (a) Standard Case (a) Standard Case (a) Standard Case



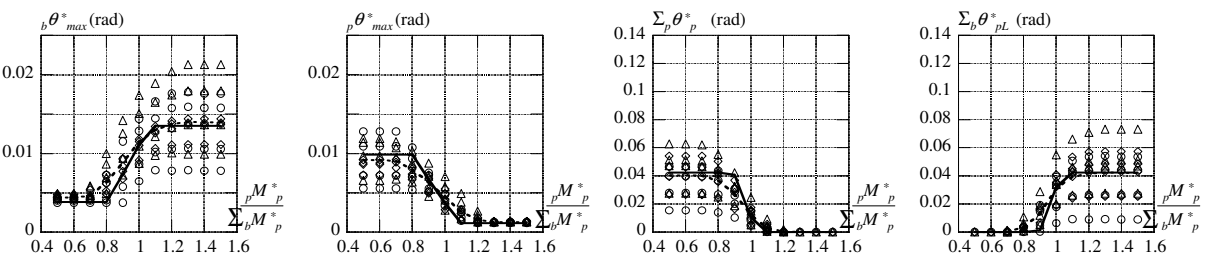
(b) $C_B = 0.24$ (b) $C_B = 0.24$ (b) $C_B = 0.24$ (b) $C_B = 0.24$



(c) $bM_{pL}^*/bM_{pR}^* = 0.5$ (c) $bM_{pL}^*/bM_{pR}^* = 0.5$ (c) $bM_{pL}^*/bM_{pR}^* = 0.5$ (c) $bM_{pL}^*/bM_{pR}^* = 0.5$



(d) $bK_L = 0.7$ (d) $bK_L = 0.7$ (d) $bK_L = 0.7$ (d) $bK_L = 0.7$



(e) $\rho K^*/bK^* = 3.0$ (e) $\rho K^*/bK^* = 3.0$ (e) $\rho K^*/bK^* = 3.0$ (e) $\rho K^*/bK^* = 3.0$

Figure 12. $b\theta_{max}^*$

Figure 13. $\rho\theta_{max}^*$

Figure 14. $\sum b\theta_{pL}^*$

Figure 15. $\sum \rho\theta_p^*$